metals

MDPI

Article

The Role of Silica in the Chlorination–Volatilization of Cobalt Oxide by Using Calcium Chloride

Peiwei Han [1,2,*], Zhengchen Li [1,2], Xiang Liu [1,2], Jingmin Yan [1,2] and Shufeng Ye [1,2,*]

[1] State Key Laboratory of Multiphase Complex Systems, Institute of Process Engineering, Chinese Academy of Sciences, Beijing 100190, China; lizhengchen19@ipe.ac.cn (Z.L.); liuxiang@ipe.ac.cn (X.L.); 18813095233@163.com (J.Y.)

[2] Innovation Academy for Green Manufacture, Chinese Academy of Sciences, Beijing 100190, China

* Correspondence: pwhan@ipe.ac.cn (P.H.); sfye@ipe.ac.cn (S.Y.); Tel.: +86-13811635732; (P.H.); +86-13911828468 (S.Y.)

Abstract: The role of silica in the chlorination–volatilization of cobalt oxide, using calcium chloride, is investigated in this paper. It is found that the Co volatilization percentage of the CoO–Fe_2O_3–$CaCl_2$ system is not larger than 12.1%. Silica plays an important role in the chlorination–volatilization of cobalt oxide by using calcium chloride. In the CoO–SiO_2–Fe_2O_3–$CaCl_2$ system, the Co volatilization percentage is initially positively related to the molar ratio of SiO_2 to $CaCl_2$, and remains almost constant when the molar ratio of SiO_2 to $CaCl_2$ rises from zero to eight. The critical molar ratios of SiO_2 to $CaCl_2$ are 1 and 2 when the molar ratios of $CaCl_2$ to CoO are 8.3 and 16.6, respectively. The Co volatilization percentage remains almost constant with the increase in CaO concentration, and decreases when Al_2O_3 and MgO are added. $Ca_2SiO_3Cl_2$ is determined after roasting at 1073 K and 1173 K, and disappears at temperatures in excess of 1273 K in the calcines from the CoO–SiO_2–$CaCl_2$ system. $CaSiO_3$ always exists in the calcines at temperatures in excess of 973 K.

Keywords: chlorination–volatilization; cobalt oxide; calcium chloride; phases of calcines

Citation: Han, P.; Li, Z.; Liu, X.; Yan, J.; Ye, S. The Role of Silica in the Chlorination–Volatilization of Cobalt Oxide by Using Calcium Chloride. *Metals* **2021**, *11*, 2036. https://doi.org/10.3390/met11122036

Academic Editors: Baojun Zhao, Jianliang Zhang, Xiaodong Ma and Felix A. Lopez

Received: 10 November 2021
Accepted: 10 December 2021
Published: 15 December 2021

1. Introduction

When roasted at a high temperature, nonferrous metal oxides are converted into corresponding chlorides and volatilize in the form of gaseous chlorides in the presence of chlorinating agents. The chlorination–volatilization method has been used for the recovery of valuable metals from slags or refractory ores, such as Au, Ag, Cu, Pb, and Zn [1–6].

In regards to cobalt recovery, many works have concentrated on chloride roasting as the pretreatment to convert cobalt compounds into soluble chloride, followed by a subsequent hydrometallurgical step [7–14]. The chloridizing agents used for chloride roasting include gaseous Cl_2 and HCl, and solid $MgCl_2 \bullet 6H_2O$, NaCl, $AlCl_3 \bullet 6H_2O$, and NH_4Cl. However, there are few investigations about the chlorination–volatilization of cobalt at present. It was reported that to obtain approximately 50% volatilization percentage, a chlorine consumption of approximately 2.5 times the stoichiometric amount was needed, in the case of producing iron ore pellets from pyrite cinders containing nonferrous metals by using chlorine [15].

Calcium chloride is a popular chloridizing agent because of its high stability and lack of toxicity in practice. The chlorination–volatilization of cobalt, using calcium chloride, was investigated in our previous paper [16]. The effects of different variables on the cobalt volatilization percentage were investigated, including flow rate, oxygen partial pressure and water vapor content of the carrier gas, roasting time, and temperature. The aims of this paper are to investigate the effects of silica, other gangues (Al_2O_3, CaO, and MgO) and $CaCl_2$ dosage on the Co volatilization percentages during the chlorination–volatilization of cobalt oxide, and on the phases of calcines after roasting.

2. Materials and Methods

Cobalt-containing slags were prepared using reagent-grade CoO, SiO_2, Fe_2O_3, Al_2O_3, MgO and CaO powders. Reagent-grade anhydrous $CaCl_2$ was adopted as the chlorinating agent. All the reagents were precisely weighed according to the compositions shown in Table 1 and pressed into briquettes after sufficient mixing. The effects of $CaCl_2$ dosage on the Co volatilization percentage were investigated from No.1 to No.5. The effects of the molar ratio of SiO_2 to $CaCl_2$ on the Co volatilization percentage were also investigated from No.4 to No.14. Finally, the effects of Al_2O_3, MgO and CaO additions on the Co volatilization percentage were investigated from No.14 to No.20.

Table 1. Sample compositions and $CaCl_2$ dosage.

No.	Slag Composition (Mass%)						$CaCl_2$ Dosage (Mass%)	Molar Ratio of $CaCl_2$ to CoO	Molar Ratio of SiO_2 to $CaCl_2$
	CoO	SiO_2	Al_2O_3	MgO	CaO	Fe_2O_3			
1	1	0	0	0	0	99	12.3	8.3	0
2	1	0	0	0	0	99	18.5	12.5	0
3	1	0	0	0	0	99	24.6	16.6	0
4	1	99	0	0	0	0	12.3	8.3	14.9
5	1	99	0	0	0	0	24.6	16.6	7.7
6	1	6.66	0	0	0	92.34	24.6	16.6	0.5
7	1	13.33	0	0	0	85.67	24.6	16.6	1
8	1	26.66	0	0	0	72.34	24.6	16.6	2
9	1	53.31	0	0	0	45.69	24.6	16.6	4
10	1	3.33	0	0	0	95.67	12.3	8.3	0.5
11	1	6.66	0	0	0	92.34	12.3	8.3	1
12	1	13.33	0	0	0	85.67	12.3	8.3	2
13	1	26.66	0	0	0	72.34	12.3	8.3	4
14	1	53.31	0	0	0	45.69	12.3	8.3	8
15	1	53.31	10	0	0	35.69	12.3	8.	8
16	1	53.31	20	0	0	25.69	12.3	8.3	8
17	1	53.31	0	10	0	35.69	12.3	8.3	8
18	1	53.31	0	20	0	25.69	12.3	8.3	8
19	1	53.31	0	0	10	35.69	12.3	8.3	8
20	1	53.31	0	0	20	25.69	12.3	8.3	8

The chlorination–volatilization experiments were carried out in a muffle furnace. Furnace temperature was set to increase at 25 K/min. An alumina boat (length: 60 mm, width: 30 mm) containing approximately 10 g of briquettes was located at the center of the furnace at approximately 873 K. The furnace was turned off after the sample was held at the desired temperatures for 1 h, which was sufficient to reach the maximum cobalt volatilization percentage according to previous work [16]. There was an air inlet under the thermocouple and an air outlet at the top of the furnace hearth to connect with the atmosphere. Hot air in the furnace hearth escaped through the outlet and was exhausted by a negative pressure fan above the furnace into the air after alkaline solution treatment. Samples were cooled inside the furnace to approximately 873 K and then naturally cooled to room temperature.

Samples after roasting were prepared carefully for the chemical and phase analyses. The phases of calcines were detected by X-ray diffraction (XRD, X'PertPro, PANalytical, Almelo, The Netherlands) and identified by comparisons between diffraction peaks of XRD data and no less than three main characteristic peaks of substances. Cobalt concentration was measured by inductively coupled plasma optical emission spectrometer (ICP-OES, Optima 8000, PerkinElmer, Waltham, Massachusetts, MA, USA). The Co volatilization percentage was calculated according to Equation (1).

$$\eta = \frac{c_i m_i - c_f m_f}{c_i m_i} \times 100\%, \quad (1)$$

where c_i and c_f are Co concentrations of samples before and after roasting, respectively. m_i and m_f are the masses of the samples before and after roasting, respectively. The analysis results of cobalt concentrations are within ± 0.015 mass%. Therefore, the errors of volatilization percentages are calculated to be within $\pm 2.5\%$ according to Equation (1).

3. Results and Discussions

3.1. Effect of $CaCl_2$ Dosage

Figure 1 shows the effect of $CaCl_2$ dosage on Co volatilization percentage in the CoO–Fe_2O_3–$CaCl_2$ and CoO–SiO_2–$CaCl_2$ systems. The Co volatilization percentage obviously increases as the $CaCl_2$ dosage in the CoO–SiO_2–$CaCl_2$ system is strengthened at 1173 K, and slightly increases with increasing $CaCl_2$ dosage at 1273 K and 1373 K. Similar trends are observed in the CoO–Fe_2O_3–$CaCl_2$ system. It should be noted that the Co volatilization percentages in the CoO–SiO_2–$CaCl_2$ system are much larger than those in the CoO–Fe_2O_3–$CaCl_2$ system.

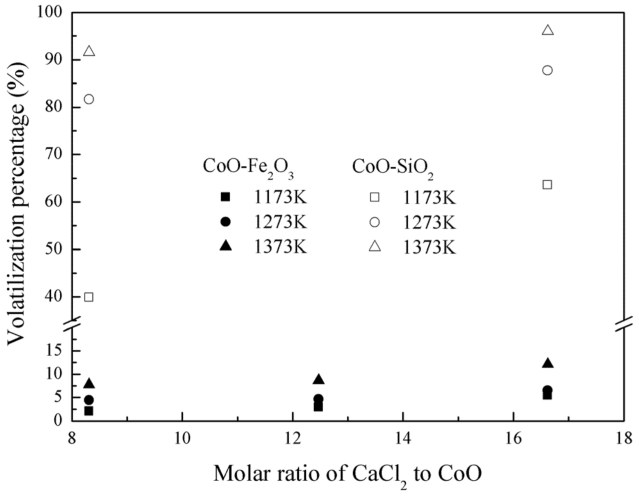

Figure 1. Effect of $CaCl_2$ dosage on the Co volatilization percentage.

Chlorination could be divided into direct chlorination and indirect chlorination using calcium chloride. It reacts directly with cobalt oxide in the former case, which could be represented as follows:

$$CaCl_2 + CoO = CoCl_2 + CaO, \quad (2)$$

$CaCl_2$ firstly reacts with oxygen to release Cl_2 in the latter case, followed by cobalt oxide being chlorinated by Cl_2. It could be expressed as follows:

$$2CaCl_2 + O_2 = 2CaO + 2Cl_2, \quad (3)$$

$$2CoO + 2Cl_2 = 2CoCl_2 + O_2, \quad (4)$$

Figure 1 shows that the Co volatilization percentage of the CoO–Fe_2O_3–$CaCl_2$ system is not larger than 12.1%, even with a higher $CaCl_2$ dosage, and it becomes much larger in the CoO–SiO_2–$CaCl_2$ system. This indicates that SiO_2 is more beneficial to the chlorination–volatilization of cobalt oxide compared with Fe_2O_3 in both the cases of direct and indirect chlorination. The direct chlorination of cobalt oxide by calcium chloride, in the presence of SiO_2, could be expressed as follows:

$$CaCl_2 + CoO + SiO_2 = CoCl_2 + CaSiO_3, \quad (5)$$

The generation of Cl_2 by the decomposition of $CaCl_2$, in the presence of SiO_2, could be expressed as follows:

$$2CaCl_2 + O_2 + 2SiO_2 = 2CaSiO_3 + 2Cl_2, \quad (6)$$

The standard Gibbs free energies of Equations (2)–(6) are calculated according to the data from [17], and are shown in Figure 2. Equations (7)–(9) in Section 3.4 are also listed in Figure 2. $CoCl_2$ is considered to be in the gaseous state. The standard Gibbs free energies

of Equations (5) and (6) are much lower than those of Equations (2) and (3), respectively, which means that the chlorination of cobalt oxide is promoted in the presence of SiO_2. A larger $CaCl_2$ dosage is helpful to improve the Co volatilization percentage in the presence of SiO_2 in both the cases of direct and indirect chlorination.

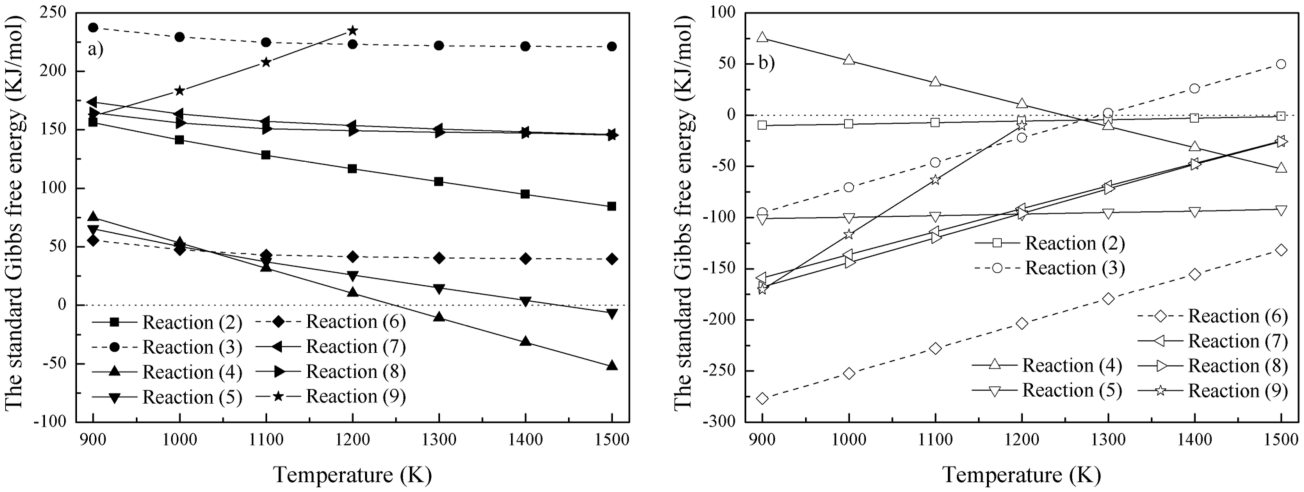

Figure 2. The standard Gibbs free energy of reactions: (**a**) solid or liquid $CaCl_2$; (**b**)gaseous $CaCl_2$.

3.2. Effect of the Molar Ratio of SiO_2 to $CaCl_2$

Figure 3 shows the effect of the molar ratio of SiO_2 to $CaCl_2$ on the Co volatilization percentage in the CoO–SiO_2–Fe_2O_3–$CaCl_2$ system. When the molar ratio of $CaCl_2$ to CoO is 8.3, the Co volatilization percentage increases significantly, as the molar ratio of SiO_2 to $CaCl_2$ rises from 0 to 1, and remains almost constant when the molar ratio of SiO_2 to $CaCl_2$ increases from 1 to 8 at all the desired temperatures. Similar trends are observed when the molar ratio of $CaCl_2$ to CoO is 16.6 at 1273 K and 1373 K. The Co volatilization percentage increases significantly and remains almost constant when the critical molar ratio of SiO_2 to $CaCl_2$ is two. However, it increases significantly as the molar ratio of SiO_2 to $CaCl_2$ is amplified at 1173 K.

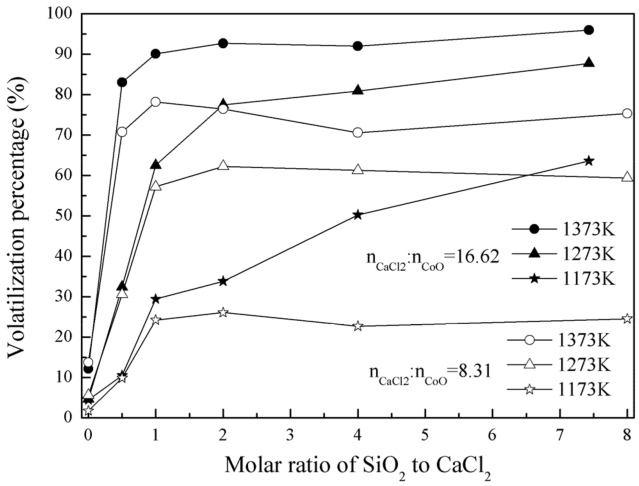

Figure 3. Effect of the molar ratio of SiO_2 to $CaCl_2$ on the Co volatilization percentage.

Equation (5) is initially promoted with an increase in the molar ratio of SiO_2 to $CaCl_2$ from zero. The enhancement becomes weaker when the molar ratio of SiO_2 to $CaCl_2$ is large enough. As shown in Equation (6), SiO_2 plays an important role in the generation of

Cl_2, by the decomposition of $CaCl_2$. This result is consistent with the works of Liu et al. [18], Zhu et al. [19], and Ding [20]. The Co volatilization percentage is very low when the molar ratio of SiO_2 to $CaCl_2$ is zero. Most of the $CaCl_2$ is lost in the form of volatilization in this case. This also means that the role of Fe_2O_3 in the generation of Cl_2, by the decomposition of $CaCl_2$, is much weaker than that of SiO_2. More Cl_2 is released when the molar ratio of SiO_2 to $CaCl_2$ is increased, which leads to an increase in the Co volatilization percentage. There is sufficient Cl_2 at a high molar ratio of SiO_2, resulting in a constant Co volatilization percentage.

3.3. Effect of Al_2O_3, MgO and CaO

Figure 4 shows the effects of Al_2O_3, MgO, and CaO on the Co volatilization percentage in the CoO–SiO_2–(Al_2O_3/MgO/CaO)–Fe_2O_3–$CaCl_2$ systems. The Co volatilization percentage remains almost constant with increasing CaO concentration, with a molar ratio of $CaCl_2$ to CoO of 8.3 and a molar ratio of SiO_2 to $CaCl_2$ of eight. This could be attributed to the sufficient amount of SiO_2 existing in the system. The molar ratio of SiO_2 to $CaCl_2$ is still larger than two, taking into consideration that some SiO_2 could react with CaO. However, it decreases with increasing Al_2O_3 and MgO concentrations under the same conditions. The reasons for this need further study. Table 2 shows the comparisons of the effects of Al_2O_3, MgO, CaO, and SiO_2 on the volatilization percentages of CoO, ZnO [19], Zn•Fe_2O_3 [19], Cu_2O [21], and CuO [21]. It should be noted that the molar ratios of $CaCl_2$ to ZnO, $CaCl_2$ to Zn•Fe_2O_3, $CaCl_2$ to Cu_2O, and $CaCl_2$ to CuO are much lower than the molar ratio of $CaCl_2$ to CoO in this study.

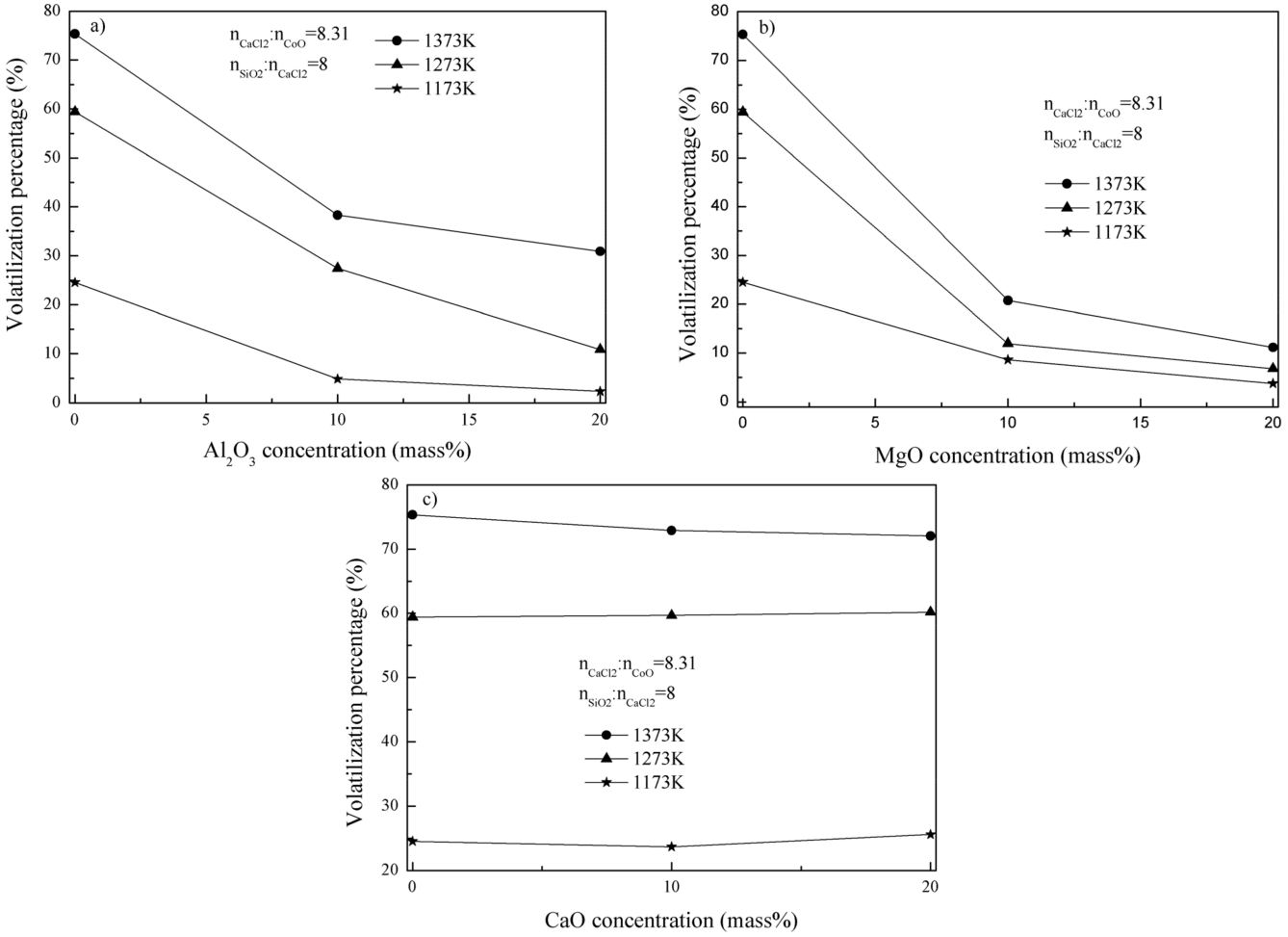

Figure 4. Effect of (**a**) Al_2O_3, (**b**) MgO and (**c**) CaO on Co volatilization percentage.

Table 2. The effects of Al_2O_3, MgO, CaO and SiO_2 on the volatilization percentage.

Phases	System	Al_2O_3	MgO	CaO	SiO_2	Reference
CoO	CoO–SiO_2–Fe_2O_3–Al_2O_3–$CaCl_2$ CoO–SiO_2–Fe_2O_3–MgO–$CaCl_2$ CoO–SiO_2–Fe_2O_3–CaO–$CaCl_2$ CoO–SiO_2–Fe_2O_3–$CaCl_2$	Negatively	Negatively	None	Positively	**This study**
ZnO	ZnO–Fe_2O_3–Al_2O_3–$CaCl_2$ ZnO–Fe_2O_3–MgO–$CaCl_2$ ZnO–Fe_2O_3–CaO–$CaCl_2$ ZnO–Fe_2O_3–SiO_2–$CaCl_2$	Negatively	Negatively	Positively	Positively	[19]
Zn•Fe_2O_3	Zn•Fe_2O_3–Fe_2O_3–Al_2O_3–$CaCl_2$ Zn•Fe_2O_3–Fe_2O_3–MgO–$CaCl_2$ Zn•Fe_2O_3–Fe_2O_3–CaO–$CaCl_2$ Zn•Fe_2O_3–Fe_2O_3–SiO_2–$CaCl_2$	Negatively	Negatively	Negatively	Negatively	[19]
Cu_2O	Cu_2O–Fe_2O_3–Al_2O_3–$CaCl_2$ Cu_2O–Fe_2O_3–MgO–$CaCl_2$ Cu_2O–Fe_2O_3–CaO–$CaCl_2$ Cu_2O–Fe_2O_3–SiO_2–$CaCl_2$	Negatively	Negatively	Negatively	Negatively	[21]
CuO	CuO–Fe_2O_3–Al_2O_3–$CaCl_2$ CuO–Fe_2O_3–MgO–$CaCl_2$ CuO–Fe_2O_3–CaO–$CaCl_2$ CuO–Fe_2O_3–SiO_2–$CaCl_2$	None	Negatively	Positively	Positively	[21]

3.4. Phases of Calcines

Figure 5 shows the XRD results of the calcines from the CoO–Fe_2O_3–$CaCl_2$ system after roasting with a molar ratio of $CaCl_2$ to CoO of 16.6. Fe_2O_3, $CaFe_2O_4$, $Ca_2Fe_2O_5$, and $CaCO_3$ are identified in the calcines at 973 K, which is a temperature lower than the melting point of $CaCl_2$ (1055 K). The diffraction peaks of $CaCO_3$ disappear at temperatures higher than 1173 K, which could be attributed to the decomposition of $CaCO_3$. The generation of Cl_2, by the decomposition of $CaCl_2$, in the CoO–Fe_2O_3–$CaCl_2$ system could be expressed as follows:

$$2CaCl_2 + O_2 + Fe_2O_3 = Ca_2Fe_2O_5 + 2Cl_2, \quad (7)$$

$$2CaCl_2 + O_2 + 2Fe_2O_3 = 2CaFe_2O_4 + 2Cl_2, \quad (8)$$

$$2CaCl_2 + O_2 + 2CO_2 = 2CaCO_3 + 2Cl_2, \quad (9)$$

where Equation (9) occurs at temperatures no more than 1173 K. The equilibrated chlorine partial pressure of Equation (9) is calculated according to Equation (10), and is shown in Figure 6, where the O_2 and CO_2 partial pressures are 0.209 and 3.1×10^{-4}, respectively. The chlorine partial pressure is approximately 10^{-9} when the activity of solid or liquid $CaCl_2$ is set to one. This means that Equation (9) could theoretically take place when the chlorine partial pressure is less than 10^{-9}. The equilibrated chlorine partial pressure becomes much larger when $CaCl_2$ changes from the solid or liquid state to the gaseous state.

$$\frac{\Delta G_9^0}{-RT} = \ln \frac{(P_{Cl_2}/P^0)^2}{a_{CaCl_2}(P_{CO_2}/P^0)^2(P_{O_2}/P^0)^{0.5}} or = \ln \frac{(P_{Cl_2}/P^0)^2}{(P_{CaCl_2}/P^0)^2(P_{CO_2}/P^0)^2(P_{O_2}/P^0)^{0.5}} \quad (10)$$

Figure 7 shows the XRD results of the calcines from the CoO–SiO_2–$CaCl_2$ system after roasting with a molar ratio of $CaCl_2$ to CoO of 16.6. There is newly generated $CaSiO_3$, and unreacted SiO_2 and $CaCl_2$, at 973 K. Newly generated $Ca_2SiO_3Cl_2$ exists alongside $CaSiO_3$ at 1073 K and 1173 K. The formation reaction of $Ca_2SiO_3Cl_2$ could be expressed as follows:

$$4CaCl_2 + O_2 + 2SiO_2 = 2Ca_2SiO_3Cl_2 + 2Cl_2, \quad (11)$$

The diffraction peaks of $Ca_2SiO_3Cl_2$ disappear at temperatures in excess of 1273 K, and only newly generated $CaSiO_3$ and unreacted SiO_2 remain in the calcines. This could be attributed to the instability of $Ca_2SiO_3Cl_2$ at higher temperatures. The reaction could be expressed as follows:

$$2Ca_2SiO_3Cl_2 + O_2 + 2SiO_2 = 4CaSiO_3 + 2Cl_2, \quad (12)$$

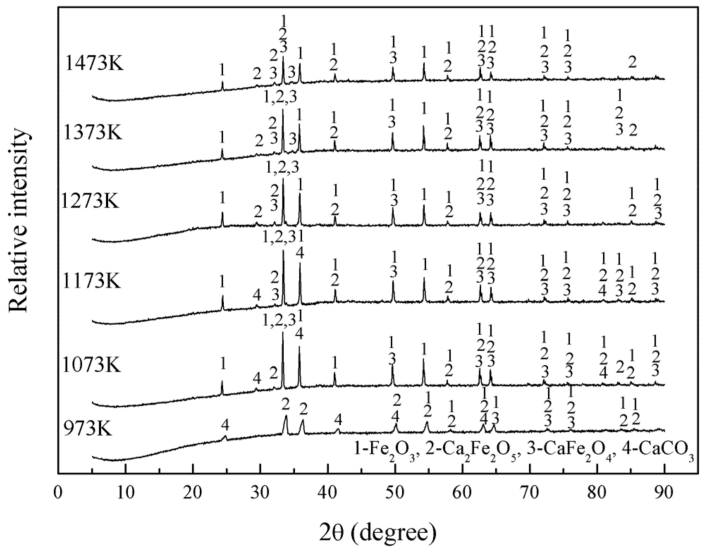

Figure 5. XRD results of calcines from the CoO–Fe_2O_3–$CaCl_2$ system.

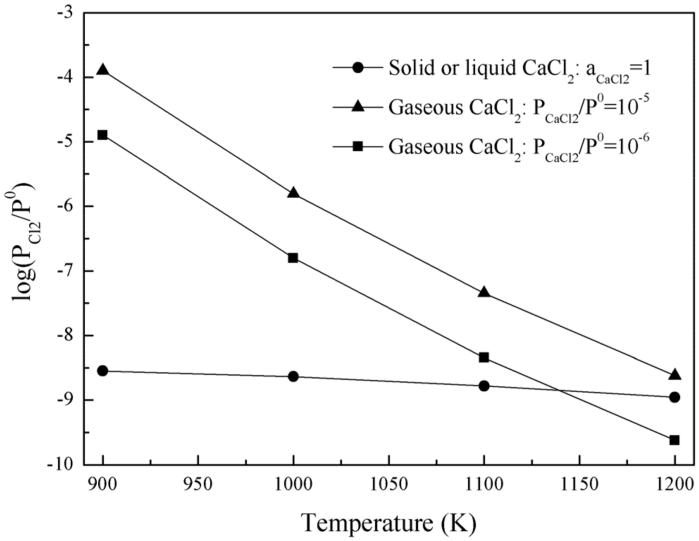

Figure 6. The equilibrated chlorine partial pressure of the following reaction: $2CaCl_2 + O_2 + 2CO_2 = 2CaCO_3 + 2Cl_2$.

$Ca_2SiO_3Cl_2$ was formed when the molar ratios of SiO_2 to $CaCl_2$ were two and one at 1023 K and 1073 K, respectively [22]. In this study, $Ca_2SiO_3Cl_2$ is formed when the molar ratio of SiO_2 to $CaCl_2$ is approximately 7.4 at 1073 K and 1173 K. Considering the results presented by Zhang [22], along with those from this study, it is suggested that the intermediate product $Ca_2SiO_3Cl_2$ is formed when the molar ratio of SiO_2 to $CaCl_2$ is larger than one at temperatures between 1023 K and 1173 K.

$CaSiO_3$, $CaFe_2O_4$, $Ca_2Fe_2O_5$, and $Ca_3Fe_2(SiO_4)_3$ are generated in the CoO–SiO_2–Fe_2O_3–$CaCl_2$ system at 1273 K, with a molar ratio of $CaCl_2$ to CoO of 8.3 and a molar ratio of SiO_2 to $CaCl_2$ of eight [16]. $CaAl_2Si_2O_8$ and $CaMg(SiO_3)_2$ are generated after the addition of Al_2O_3 and MgO, respectively, as shown in Figure 8.

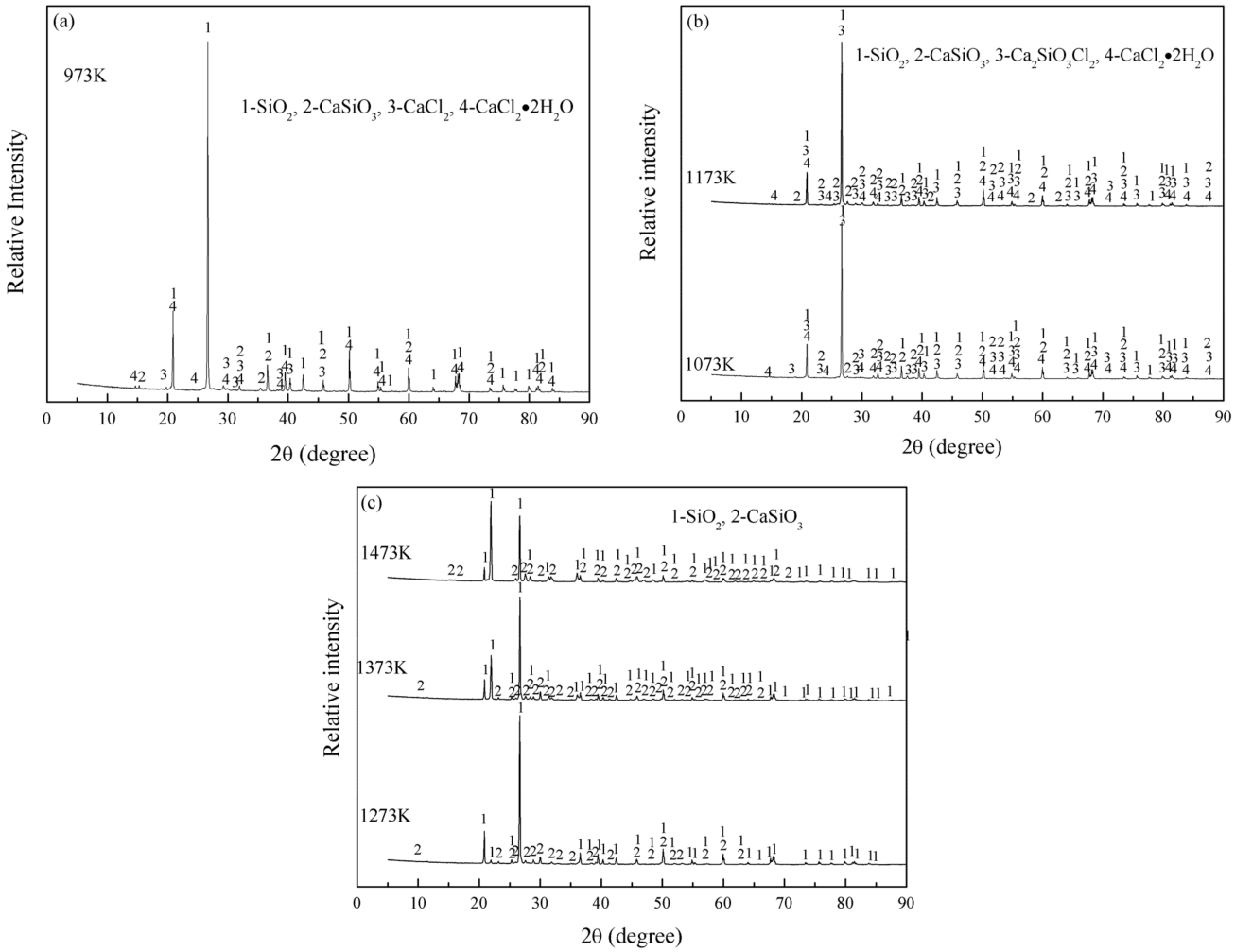

Figure 7. XRD results of calcines from the $CoO–SiO_2–CaCl_2$ system (**a**) at 973 K; (**b**) at 1073 K and 1173 K; (**c**) between 1273 K and 1473 K.

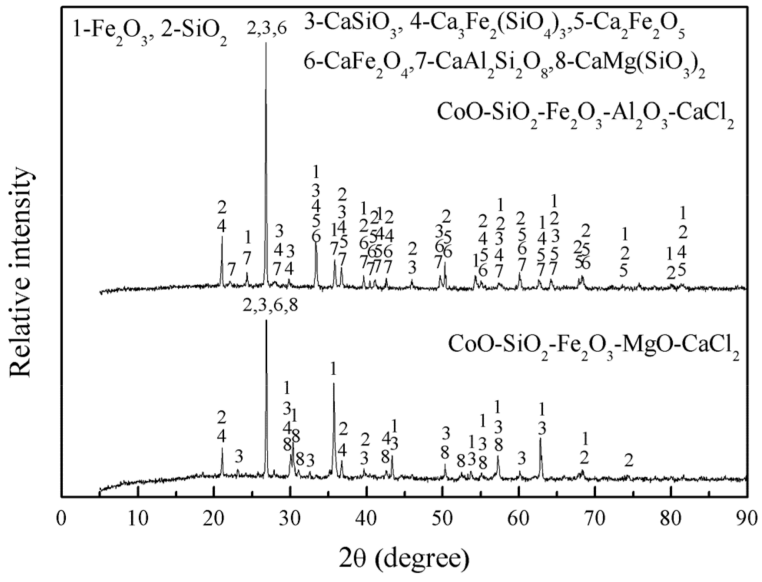

Figure 8. XRD results of calcines from the $CoO–SiO_2–Fe_2O_3–(Al_2O_3/MgO)–CaCl_2$ system at 1273 K.

4. Conclusions

The following conclusions could be drawn from this study:

1. The Co volatilization percentage of the CoO–Fe_2O_3–$CaCl_2$ system is not larger than 12.1%.
2. SiO_2 plays an important role in the chlorination–volatilization of cobalt oxide, using calcium chloride. In the CoO–SiO_2–Fe_2O_3–$CaCl_2$ system, the Co volatilization percentage is initially positively related to the molar ratio of SiO_2 to $CaCl_2$, and remains almost constant when the molar ratio of SiO_2 to $CaCl_2$ rises from zero to eight. The critical molar ratios of SiO_2 to $CaCl_2$ are 1 and 2 when the molar ratios of $CaCl_2$ to CoO are 8.3 and 16.6, respectively.
3. The Co volatilization percentage remains almost constant with increasing CaO concentration, and decreases when Al_2O_3 and MgO are added, with a molar ratio of $CaCl_2$ to CoO of 8.3 and a molar ratio of SiO_2 to $CaCl_2$ of eight.
4. Fe_2O_3, $CaFe_2O_4$, $Ca_2Fe_2O_5$, and $CaCO_3$ are identified in the calcines from the CoO–Fe_2O_3–$CaCl_2$ system at 973 K, and $CaCO_3$ disappears at temperatures higher than 1173 K.
5. $Ca_2SiO_3Cl_2$ exists in the calcines from the CoO–SiO_2–$CaCl_2$ system at 1073 K and 1173 K, and disappears at temperatures in excess of 1273 K. $CaSiO_3$ always exists in the calcines at temperatures in excess of 973 K.

Author Contributions: Methodology, P.H. and S.Y.; formal analysis, P.H.; investigation, P.H., Z.L., X.L. and J.Y.; data curation, P.H.; writing—original draft preparation, P.H.; writing—review and editing, S.Y.; supervision, S.Y.; funding acquisition, S.Y. All authors have read and agreed to the published version of the manuscript.

Funding: The authors gratefully acknowledge the research funding from the National Natural Science Foundation of China (No.51804292) and Innovation Academy for Green Manufacture, Chinese Academy of Sciences (No. IAGM-2019-A05).

Institutional Review Board Statement: Not applicable.

Informed Consent Statement: Not applicable.

Data Availability Statement: The datasets analyzed or generated during the study are available from the corresponding author on reasonable request.

Conflicts of Interest: The authors declare no conflict of interest.

References

1. Jena, P.K.; Brocchi, E.A. Metal extraction through chlorine metallurgy. *Miner. Process. Extr. Metall. Rev.* **1997**, *16*, 211–237. [CrossRef]
2. Yazawa, A.; Kameda, M. The removal of impurities from pyrite cinders by a chloride volatilization process. *Can. Metall. Q.* **1967**, *6*, 263–280. [CrossRef]
3. Panias, D.; Neou-Syngouna, P. Gold extraction from pyrite cinders by high temperature chlorination. *Erzmetall* **1990**, *43*, 41–44.
4. Ojeda, M.W.; Perino, E.; Ruiz, M.C. Gold extraction by chlorination using a pyrometallurgical process. *Miner. Eng.* **2009**, *22*, 409–411. [CrossRef]
5. Guo, T.; Hu, X.; Matsuura, H.; Tsukihashi, F.; Chou, K. Kinetics of Zn removal from ZnO-Fe_2O_3-$CaCl_2$ system. *ISIJ Int.* **2010**, *50*, 1084–1088. [CrossRef]
6. Ding, J.; Han, P.; Lv, C.; Qian, P.; Ye, S.; Chen, Y. Utilization of gold-bearing and iron-rich pyrite cinder via a chlorination-volatilization process. *Int. J. Miner. Metall. Mater.* **2017**, *24*, 1241–1250. [CrossRef]
7. Gaballah, I.; Djona, M. Processing of spent hydrorefining catalysts by selective chlorination. *Metall. Mater. Trans. B* **1994**, *25*, 481–490. [CrossRef]
8. Gaballah, I.; Djona, M. Recovery of Co, Ni, Mo, and V from unroasted spent catalysts by selective chlorination. *Metall. Mater. Trans. B* **1995**, *26*, 41–50. [CrossRef]
9. Fan, C.; Zhai, X.; Fu, Y.; Chang, Y.; Li, B.; Zhang, T. Extraction of nickel and cobalt from reduced limonitic laterite using a selective chlorination—Water leaching process. *Hydrometallurgy* **2010**, *105*, 191–194. [CrossRef]
10. Fan, C.; Zhai, X.; Fu, Y.; Chang, Y.; Li, B.; Zhang, T. Kinetics of selective chlorination of pre-reduced limonitic nickel laterite using hydrogen chloride. *Miner. Eng.* **2011**, *24*, 1016–1021. [CrossRef]
11. Zhang, M.; Zhu, G.; Zhao, Y.; Feng, X. A study of recovery of copper and cobalt from copper–cobalt oxide ores by ammonium salt roasting. *Hydrometallurgy* **2012**, *129–130*, 140–144. [CrossRef]

12. Li, J.; Li, Y.; Gao, Y.; Zhang, Y.; Chen, Z. Chlorination roasting of laterite using salt chloride. *Int. J. Miner. Process.* **2016**, *148*, 23–31. [CrossRef]
13. Xu, C.; Cheng, H.; Li, G.; Lu, C.; Lu, X.; Zou, Z.; Xu, Q. Extraction of metals from complex sulfide nickel concentrates by low-temperature chlorination roasting and water leaching. *Int. J. Miner. Metall. Mater.* **2017**, *24*, 377–385. [CrossRef]
14. Cui, F.; Mu, W.; Wang, S.; Xin, H.; Shen, H.; Xu, Q.; Zhai, Y.; Luo, S. Synchronous extractions of nickel, copper, and cobalt by selective chlorinating roasting and water leaching to low-grade nickel-copper matte. *Sep. Purif. Technol.* **2018**, *195*, 149–162. [CrossRef]
15. Lippert, K.K.; Pietsch, H.B.; Roeder, A.; Walden, H.W. Recovery of non-ferrous metal impurities from iron ore pellets by chlorination (CV or LDK process). *Trans. Inst. Min. Metall. Sect. C* **1969**, *78*, 98–107.
16. Han, P.; Xiao, L.; Wang, Y.; Lu, Y.; Ye, S. Cobalt recovery by the chlorination-volatilization method. *Metall. Mater. Trans. B* **2019**, *50*, 1128–1133. [CrossRef]
17. Barin, I. *Thermochemical Data of Pure Substance*, 3rd ed.; WILEY-VCH Verlag Gmbh: Weinheim, Germany, 1995.
18. Liu, J.; Wen, S.; Chen, Y.; Liu, D.; Bai, S.; Wu, D. Process optimization and reaction mechanism of removing copper from an Fe-rich pyrite cinder using chlorination roasting. *J. Iron Steel Res. Int.* **2013**, *20*, 20–26. [CrossRef]
19. Zhu, D.; Chen, D.; Pan, J.; Zheng, G. Chlorination behaviors of zinc phases by calcium chloride in high temperature oxidizing-chloridizing roasting. *ISIJ Int.* **2011**, *51*, 1773–1777. [CrossRef]
20. Ding, J. Research on the Extraction of Gold from Gold-Bearing Pyrite Cinder by High-Temperature Chlorination Method. Ph.D. Thesis, University of Chinese Academy of Sciences, Beijing, China, 2018.
21. Zhu, D.; Chen, D.; Pan, J.; Chun, T.; Zheng, G.; Zhou, X. Chlorination behaviors of copper phases by calcium chloride in high temperature oxidizing-chloridizing roasting. In Proceedings of the 3rd International Symposium on High-Temperature Metallurgical Process, Orlando, FL, USA, 11–15 March 2012.
22. Zhang, L. Research on the Chloridizing Segregation Process of Nickel Laterites. Master's Thesis, Central South University, Changsha, China, 2011.